

## RECOMBINATION DYNAMICS IN STRAINED $\text{In}_{1-x}\text{Ga}_x\text{As}/\text{InP}$ -QUANTUM WELL STRUCTURES

A. Hoffmann, H. Siegle, L. Eckey, B. Lummer, P. Thurian, and R. Heitz  
 Institut für Festkörperphysik, TU Berlin, Hardenbergstr. 36, 10623 Berlin, Germany

B. K. Meyer, C. Wetzel, and D. M. Hofmann  
 Physikdepartment, E 16, TU München, 85748 Garching, Germany

V. Härle, F. Scholz  
 4. Physikal. Institut, Universität Stuttgart, Pfaffenwaldring 57, 70569 Stuttgart, Germany

A. Kohl  
 Institut für Halbleitertechnik, RWTH Aachen, Sommerfeldstr. 24, 52074 Aachen, Germany

(Received 22 August 1994)

We present a comprehensive study of the excitonic recombination lifetime in strained and unstrained  $\text{In}_{1-x}\text{Ga}_x\text{As}/\text{InP}$ -quantum well structures as a function of well width and Ga mole fraction. In the lattice-matched case a minimum lifetime of 650ps is observed for a well thickness of 2nm. For widths larger as well as smaller than 2nm the lifetime increases. In strained  $\text{In}_{1-x}\text{Ga}_x\text{As}/\text{InP}$  quantum wells the recombination lifetime shows a strong dependence on the Ga content. While the lifetime is nearly constant in the compressively strained case ( $x_{\text{Ga}} < 0.47$ ), we observe a drastic increase with rising Ga content for tensile strain ( $x_{\text{Ga}} > 0.47$ ).

### 1. Introduction

$\text{InGaAs}$  quantum well structures lattice matched to  $\text{InP}$  have attracted considerable attention over the last years. Various fields of applications, for instance in optoelectronics, opened up and turned the  $\text{InGaAs}/\text{InP}$  system to a subject of extensive investigations [1]. Modern epitaxial methods allow the growth of mismatched  $\text{In}_{1-x}\text{Ga}_x\text{As}$  layers below the critical thickness without interfering incorporation of defects [2]. By controlling the Ga mole fraction and proper choice of the substrate material band gap and even band structure engineering have become made possible. For instance, compressively strained  $\text{In}_{1-x}\text{Ga}_x\text{As}$  has a heavy hole (hh) valence band shifted to energies higher than the light hole (lh) band, accompanied by a decrease of the hh effective mass. This is applied in the design of high speed devices [3]. Additionally, the lower hh mass implies a reduced density of states so that laser devices based on compressively strained  $\text{In}_{1-x}\text{Ga}_x\text{As}/\text{InP}$  quantum wells reach inversion at lower carrier densities, resulting in lower threshold currents [3,4]. Tensile strain in this system may also result in lower threshold currents as was predicted by Sugawara et al. [5]. This corresponds well to the case of  $\text{InGaAs}/\text{InGaAsP}$

where threshold currents were reduced for both compressive and tensile strains [6,7].

While recombination dynamics in lattice-matched  $\text{InGaAs}/\text{InP}$  quantum wells has been subject to extensive investigations both experimental and theoretical [8], only little is known about the recombination dynamics in strained  $\text{In}_{1-x}\text{Ga}_x\text{As}/\text{InP}$  quantum wells.

The present contribution deals with the changes in the recombination lifetime that are induced by the composition- and, therefore, strain-dependent modified band structure in  $\text{In}_{1-x}\text{Ga}_x\text{As}/\text{InP}$  quantum wells. We demonstrate that the lifetimes are influenced by the changes in band offsets as well as in the effective mass, both caused by a variation of the Ga content. The lifetime is observed to rise with an onset that strongly depends on well width.

After a brief summary of the present knowledge about the band alignment of strained  $\text{In}_{1-x}\text{Ga}_x\text{As}/\text{InP}$  epilayers we will give a description of the experimental procedures. Then we will present the results of our study of the recombination dynamics in dependence on well width and Ga content, followed by a discussion.

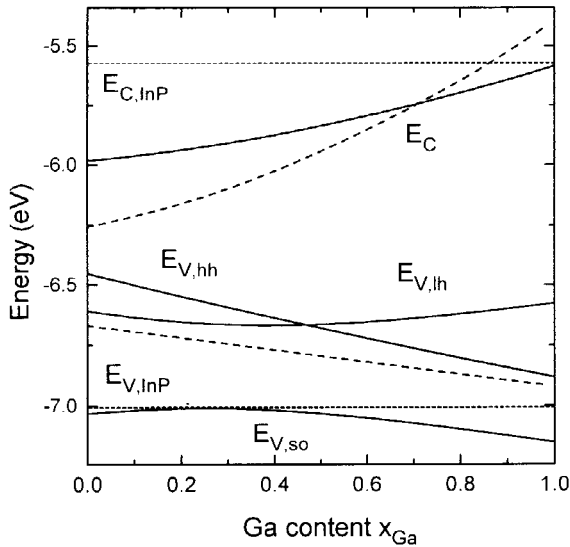


Fig. 1. Calculated band alignment of an  $\text{In}_{1-x}\text{Ga}_x\text{As}/\text{InP}$  epilayer as a function of Ga content. Dashed lines indicate the development of the conduction and valence bands without strain. The dotted lines represent the position of the InP band edges.

## 2. Band Alignment

For an understanding of the results discussed in this contribution it is necessary to summarize the state of knowledge about the band alignment in the  $\text{In}_{1-x}\text{Ga}_x\text{As}/\text{InP}$  system.

Fig. 1 presents the results of a band structure calculation of an  $\text{In}_{1-x}\text{Ga}_x\text{As}$  epilayer pseudomorphic to InP. Strain effects on the band lineups were calculated using a deformation potential model by Van de Walle and Martin [9], based on prior work by Wang and Stringfellow [10]. The position of the  $\text{In}_{1-x}\text{Ga}_x\text{As}$  valence and conduction band edges are plotted as a function of the Ga content. A calculation neglecting strain, with hh and lh bands degenerate, is indicated by dashed lines. The positions of the InP band edges are represented by dotted lines. Two effects on the respective band offsets prove important for our considerations. First, the shear strain component lifts the degeneracy of the valence bands at  $\mathbf{k}=0$ . The hh band is the highest for  $x_{\text{Ga}} < 0.47$  (compressive strain), the lh band for  $x_{\text{Ga}} > 0.47$  (tensile strain). Along with the hydrostatic strain component it causes a reduced dependency of the valence band offset on the Ga content as compared to the lattice matched case. The valence band offset is almost constant over the whole range, varying only between 550 meV for  $x_{\text{Ga}}=0$  and 430 meV for  $x_{\text{Ga}}=1$ . Second, the conduction band offset decreases monotonously with increasing  $x_{\text{Ga}}$  and vanishes for  $x_{\text{Ga}}=1$ . A staggered

alignment between the  $\text{In}_{1-x}\text{Ga}_x\text{As}$  and InP conduction bands does not appear for any  $x_{\text{Ga}}$ .

In summary, the  $\text{In}_{1-x}\text{Ga}_x\text{As}/\text{InP}$  valence band discontinuity almost remains constant over the whole range of Ga contents while that of the conduction band decreases and reaches zero for GaAs/InP.

## 3. Experimental

The samples investigated are strained and unstrained  $\text{In}_{1-x}\text{Ga}_x\text{As}/\text{InP}$  multiple and single quantum wells grown on semi-insulating InP substrates by low pressure metal-organic vapor-phase epitaxy (LP-MOVPE). We will discuss three sets of samples:

- 1) a series of lattice-matched ( $x_{\text{Ga}}=0.47$ ) single quantum wells (SQW) with well widths ranging between 0.6 and 20 nm,
- 2) a series of strained single sided p-modulation doped SQWs with varying composition ( $0.4 < x_{\text{Ga}} < 0.6$ ) and fixed well thickness of 15 nm.
- 3) a series of strained multi-quantum wells (MQW, 10 periods) with gallium contents  $0.07 < x_{\text{Ga}} < 1.00$  and nominal well thicknesses of 1.5 and 3.0 nm.

Photoluminescence measurements were performed using a He-Ne-laser ( $25\text{mW}/\text{cm}^2$ ). The emission was analyzed by a 0.75 m double grating monochromator and detected by a  $\text{LN}_2$  cooled Ge-diode. In all measurements, cw or pulsed, the samples were mounted in a He bath cryostat ( $T=1.8\text{K}$ ) or in a He gas steady-flow cryostat allowing a variation of the temperature between 8K and 300K.

Time-resolved experiments were carried out with picosecond pulses generated by a dye laser (500nm) synchronously pumped by a frequency tripled, actively mode-locked Nd:YAG laser (355nm). The overall time resolution was better than 500ps. Care was taken to adjust the excitation densities for linear excitation conditions.

## 4. Results

Fig. 2 gives the energy positions of the PL maxima as a function of the Ga content  $x_{\text{Ga}}$  for strained  $\text{In}_{1-x}\text{Ga}_x\text{As}/\text{InP}$  quantum wells 1.5 nm, 3.0 nm, and 15 nm wide. They are plotted together with the respective calculated values (full lines) which were obtained using the deformation potential model presented above. A PL spectrum of an 3 nm wide  $\text{In}_{1-x}\text{Ga}_x\text{As}/\text{InP}$ -MQW with  $x_{\text{Ga}}=0.63$  is shown in the inset of Fig. 2.

An increase of the PL maximum energy with increasing Ga content is observed for all three series of samples. For the 3 nm and 15 nm wells even the different slopes for compressive and tensile strain are resolved. For compressive strain the highest valence band is the hh band whose energy decreases while that of the conduction band

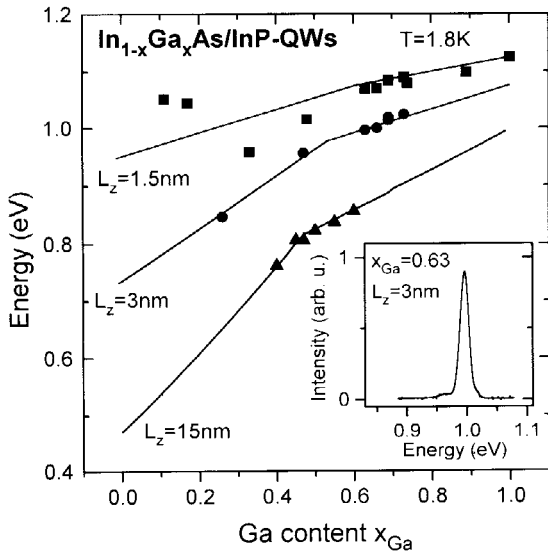


Fig. 2. Transition energies of  $In_{1-x}Ga_xAs/InP$  quantum wells for different well widths as a function of Ga content. Full lines represent calculated transition energies. The inset shows a PL spectrum of a 3nm wide  $In_{0.37}Ga_{0.63}As/InP$  quantum well.

increases with rising Ga content, resulting in a strong increase of the PL maximum energy (see also Fig. 1). For tensile strain the lh band becomes the highest valence band. In this domain conduction band and lh band exhibit a similar increase of absolute energy which leads to a much weaker slope as observed in Fig. 1.

In the following two sections we will first turn to the dynamics of the recombination in quantum wells of different widths and then investigate the dependence on the Ga content.

**4.1. Dependence of the recombination dynamics on the well width  $L_z$**

Fig. 3 is a plot of the recombination lifetime of lattice-matched  $InGaAs/InP$  quantum wells, obtained from time-resolved PL measurements, as a function of well width  $L_z$ . The lifetime decreases from 4ns for a 20nm well to a minimum of 650ps for widths between 2 and 3nm. Further decreasing the well thickness results in a rise of the lifetime back to 1.0ns for  $L_z=0.6nm$ . This is in excellent agreement with a calculation according to the model of Cebulla et al. [8], shown as a full line in Fig. 3. Details of this model are discussed below.

**4.2. Dependence on the Ga content  $x_{Ga}$**

Fig. 4 shows low temperature PL transients of three

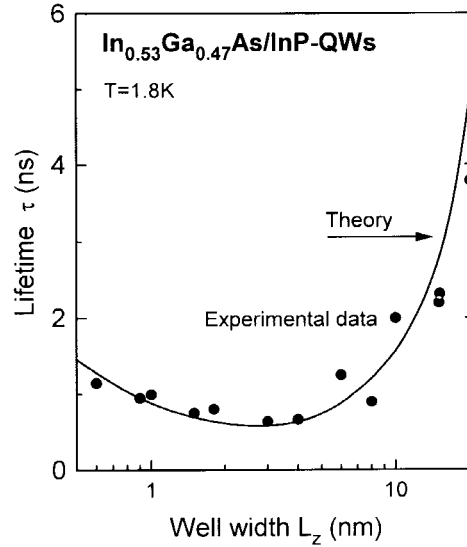


Fig. 3. Dependence of the recombination lifetime on the well width for  $In_{0.53}Ga_{0.47}As/InP$  quantum wells.

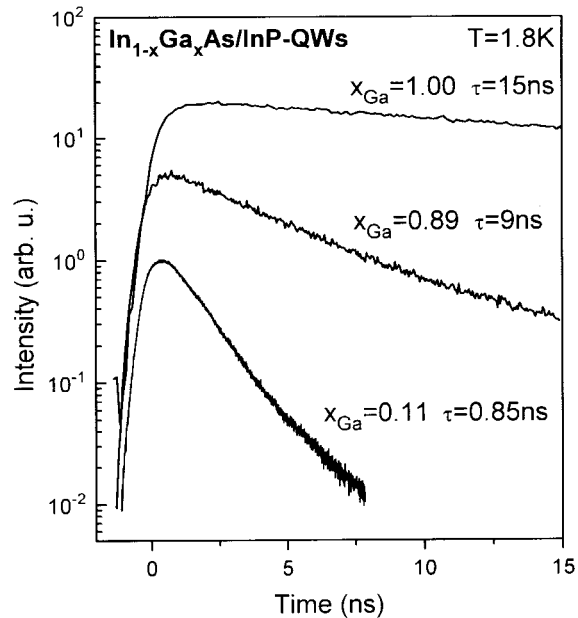


Fig. 4. Transients of 1.5nm  $In_{1-x}Ga_xAs/InP$  quantum wells for different Ga mole fractions.

strained  $In_{1-x}Ga_xAs/InP$  quantum wells with equal widths (1.5nm) but different Ga mole fractions. A rise of the recombination lifetime with increased  $x_{Ga}$  is plainly visible. A comprehensive representation of the lifetimes as a function of  $x_{Ga}$  for the strained samples is given in Fig. 5. In the domain of tensile strain we observe an onset of a rapid

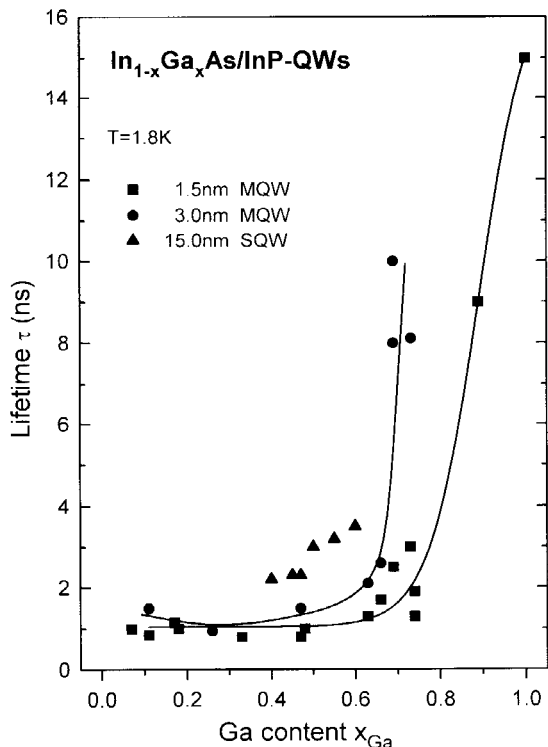


Fig. 5. Ga mole fraction dependence of the recombination lifetime for strained  $\text{In}_{1-x}\text{Ga}_x\text{As}/\text{InP}$  quantum wells. Lines are only guides to the eye.

lifetime increase leading to a maximum of 15ns. This onset is found to shift with well width from  $x_{\text{Ga}} \approx 0.74$  for 1.5nm wells down to  $x_{\text{Ga}} \approx 0.63$  for 3nm wells. For 15nm wells we see the lifetime increase as well. However, it is far less dramatic, and thus a further shift of an onset to lower values of  $x_{\text{Ga}}$  cannot be observed.

Fig. 6 gives a comparison of transients from a lattice matched sample and a strained one for temperatures between 8K and 110K. The recombination lifetime is observed to increase with temperature for the lattice-matched case, while in the strained sample it decreases between 20K and 110K.

### 5. Discussion

The dependency of the recombination lifetime on the well width is readily understood within the model by Cebulla et al. [8]:

$$\tau \propto \langle \Psi_C | \Psi_V \rangle^{-2} \cdot E_B^{-1}$$

It was also observed by Feldmann et al. [11] that first the lifetime  $\tau$  decreases with decreasing well width due to

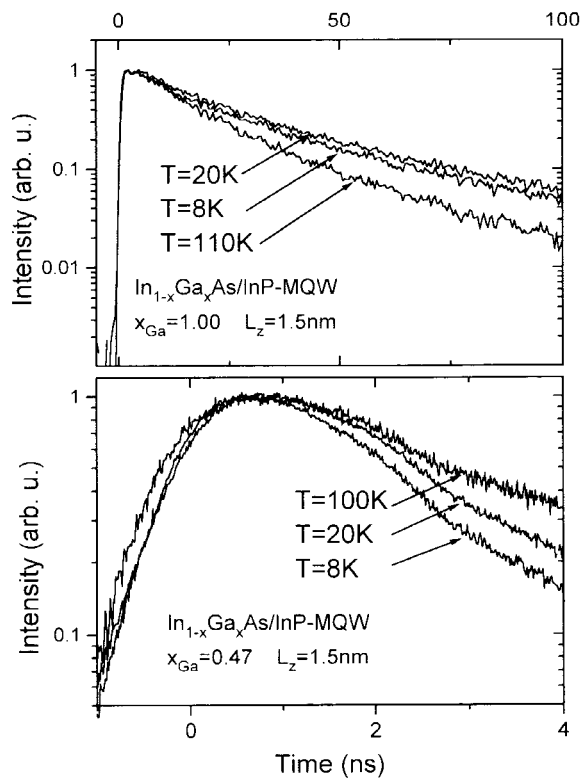


Fig. 6. Transients of a tensile strained (upper) and a lattice-matched  $\text{In}_{1-x}\text{Ga}_x\text{As}/\text{InP}$  quantum well for various temperatures.

the enhanced excitonic binding energy  $E_B$ . However, reducing the well width even further results in a smaller overlap integral of the electron and hole envelope wavefunctions  $\psi_C$  and  $\psi_V$ , respectively. For electrons penetrate stronger into the barriers than the holes which remain localised predominantly within the well. This behaviour is even more pronounced for higher ratios of the valence band to conduction band offsets.

While explaining the increase in lifetime for small well widths by the spatial separation of carriers this model principally accounts also for the observations made for different Ga mole fractions (Fig. 5).

As was discussed in section 2 the valence band offset is almost constant over the whole range of Ga contents (Fig. 1), while the conduction band offset decreases monotonously with increasing  $x_{\text{Ga}}$ . The different behaviour of the band offsets for varying Ga content becomes clear considering the ratio of the conduction band to valence band offsets which is shrinking with increased Ga content and approaching zero for  $x_{\text{Ga}}=1$  (see Fig. 7). Therefore, the potential well for electrons becomes the shallower the

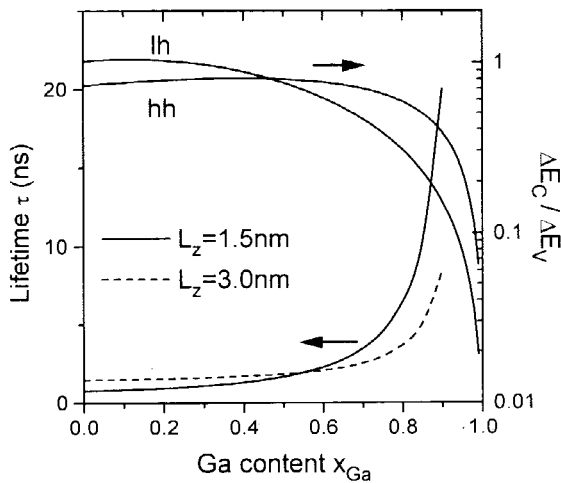


Fig. 7. Left: Calculated lifetimes of 1.5nm and 3.0nm quantum wells as a function of Ga content. Right: Calculated band offset-ratio as a function of Ga content.

higher the Ga content, thus increasing the amplitude of the electron wavefunction in the barriers. At the same time, the holes remain localized in their virtually unchanged well which leads to a reduction of the wavefunction overlap and gives rise to longer recombination lifetimes. However, our experiments show that the rise process starts at a lower  $x_{Ga}$  for 3nm quantum wells than for those with 1.5nm width, while according to this model it is expected to start at higher Ga contents (see Fig. 7). Obviously, the model has to be modified to include strain effects on the band structure. Strain induced mixing of the valence bands causes a second maximum (camel's back structure) at  $k \neq 0$  which can be higher than the one at the  $\Gamma$ -point [12]. In this case a  $k$ -indirect transition would occur with a strongly reduced transition probability giving rise to long recombination lifetimes. The camel's back structure is more pronounced for stronger mixing of valence bands. This in turn is reduced for decreasing well widths because the higher confinement energy provides for a decoupling of valence bands. So the smaller the well width the higher the Ga mole fraction necessary to create a camel's back in the valence bands, which is in agreement with our observations on 3nm and 1.5nm wells.

This point is still subject to discussions as the contradictory results of calculations made by Chao et al. [13] and Sugawara et al. [5,14] show.

The differing temperature dependencies of the lattice matched and the strained samples (Fig. 6) can be explained by the differences in band offsets. For the case of tensile strain the conduction band offset is very small (2meV). A lattice temperature of 20K already provides enough thermal energy to let the electrons surmount the potential step and scatter into the barrier. This way an additional

recombination channel is created reducing the lifetime at higher temperatures. No information about a transfer of carriers between the maxima of the camel's back of the valence band, which should shorten the recombination lifetime as well, can thus be deduced from the temperature dependencies.

## 6. Conclusion

We have presented results of time integrated and time resolved PL experiments on strained and unstrained  $In_{1-x}Ga_xAs/InP$  quantum well structures with Ga contents between 0.07 and 1.0 and well widths between 0.6nm and 20nm. The dependency of the recombination lifetime on the well width is explained using a model by Cebulla et al. The measured lifetimes can be fitted in terms of the vertical electron-hole overlap and the vertical exciton extension. An increased Ga content results in a rise of the recombination lifetime. A transfer of the Cebulla model to this situation is unsatisfactory because it cannot explain why the lifetime increase begins at smaller Ga mole fractions for larger quantum wells. Here, the impact of strain on the valence band structure has to be taken into account predicting the formation of a camel's back like structure by valence band mixing in the case of tensile strain.

## References

- [1] D. Gershoni, H. Temkin, and M. B. Panish, *Appl. Phys. Lett.* **53**, 1294 (1988)
- [2] R. People, *Appl. Phys. Lett.* **50**, 1604 (1987)
- [3] E. H. Reihlen, D. Birkedal, T. Y. Wang, G. B. Stringfellow, *J. Appl. Phys.* **68**, 1750 (1990)
- [4] E. Yablonovitch and E. O. Kane, *IEEE J. Lightwave Technol.* **LT-6**, 1202 (1988)
- [5] M. Sugawara, *Appl. Phys. Lett.* **60**, 1842 (1992)
- [6] L. F. Tiemeijer, P. J. A. Thijs, P. J. de Waard, J. J. M. Binsma, T. van Dongen, *Appl. Phys. Lett.* **58**, 2738 (1991)
- [7] P. J. A. Thijs, L. F. Tiemeijer, P. I. Kuindersma, J. J. M. Binsma, and T. van Dongen, *IEEE J. Quantum Electron.* **QE-27**, 1426 (1991)
- [8] U. Cebulla, G. Bacher, G. Mayer, A. Forchel, W. T. Tsang, M. Razeghi, *Superlatt. Microstruct.* **5**, 227 (1989)
- [9] C. G. Van de Walle and R. M. Martin, *Phys. Rev. B* **34**, 5621 (1986)
- [10] T. Y. Wang and G. B. Stringfellow, *J. Appl. Phys.* **67**, 344 (1990)
- [11] J. Feldmann, G. Peter, E. O. Göbel, P. Dawson, K. Moore, C. Fowon, R. J. Elliot, *Phys. Rev. B* **36**, 2 (1987)
- [12] E. P. O'Reilly, *Semicond. Sci. Technol.* **4**, 121 (1989)
- [13] C. Y.-P. Chao and S. L. Chuang, *Phys. Rev. B* **46**, 4110 (1992)
- [14] M. Sugawara, N. Okazaki, T. Fujii, S. Yamzaki, *Phys. Rev. B* **48**, 8102 (1993)